RSC Advances

PAPER

View Article Online
View Journal | View Issue

Cite this: *RSC Adv.*, 2022, **12**, 22180

3-(Propylthio)propane-1-sulfonic acid immobilized on functionalized magnetic nanoparticles as an efficient catalyst for one-pot synthesis of dihydrotetrazolo[1,5-*a*]pyrimidine and tetrahydrotetrazolo[5,1-*b*]quinazolinone derivatives†

Fatemeh Karimi, Behnaz Tighsazzadeh, Beheshteh Asadi, Iraj Mohammadpoor-Baltork, * Mahsa Layeghi, Valiollah Mirkhani, Shahram Tangestaninejad and Majid Moghadam

An efficient and reusable catalyst, which is 3-(propylthio)propane-1-sulfonic acid immobillized on functionalized magnetic nanoparticles [PTPSA@SiO_2–Fe_3O_4], has been synthesized. For the first time, it is highlighted under solvent-free conditions for the catalytic activity in multicomponent synthesis of dihydrotetrazolo[1,5-*a*]pyrimidines, dihydrotetrazolo[1,5-*a*]pyrimidine-6-carboxylates and tetrahydrotetrazolo[5,1-*b*]quinazolinones. The structure of the catalyst was well confirmed by characterization techniques, such as FT-IR, TGA, SEM-EDX, elemental mapping, TEM, VSM and elemental analysis. Besides, this unique catalyst was found to be effectual up to six cycles, which made it spotlighted. Recyclability of catalyst, excellent yield of the products, short reaction time and clean reaction profile are the advantages of the present protocol.

Received 21st June 2022
Accepted 29th July 2022

DOI: 10.1039/d2ra03813g

rsc.li/rsc-advances

Introduction

Owing to growing environmental concerns, the progress of a clean synthetic method has become significant and demands investigation.[1] In this context, heterogeneous organic reactions with so many advantages, such as ease of handling, recycling, separation, and environmentally-safe disposal, have attracted increasing interest.[2] Furthermore, numerous nanocatalysts have been designed and created;[3] among which, the magnetic solid acid catalysts exhibit great activity, compared to the other homogeneous and commercial catalysts. This is because of their useful properties, such as large surface area, thermal stability, biocompatibility, easy recovery in the presence of external magnetic fields, and higher loading of active sites.[4]

One of the smartest synthetic strategies to provide structurally-diverse molecules in a single reaction step is multicomponent reaction (MCR).[5] In this regard, MCR opens our hands in the synthesis of new heterocyclic frameworks with pyrimidine moiety which possesses remarkable biological activities.[6] Synthesis of dihydrotetrazolo[1,5-*a*]pyrimidines, dihydrotetrazolo[1,5-*a*]pyrimidine-6-carboxylates and tetrahydrotetrazolo[5,1-*b*]quinazolinones[7] and their derivatives have attracted attention through one-pot MCR, with huge benefits of atom economy and selectivity employing I_2/i-PrOH,[7a] $AlCl_3$/CH_3CN,[7b] nano-Fe_3O_4@SiO_2–NH-gallic acid,[7c] Fe_2O_3@SiO_2-$(CH_2)_3NHC(O)(CH_2)_2PPh_2$,[7d] Pd catalyst,[7e] TBBDA,[7f] LDH@TU-SA@Ni/DMF.[7g] However, in these cases high loadings (up to 20 mol%)[7b] of catalyst were necessary to achieve reasonably high yields. Furthermore, some of these approaches require high temperatures,[7e] harmful organic solvents,[7b,g] and non-reusable catalysts.[7a,b] consequently, development of simple and environmentally benign synthetic method for efficient preparation of these compounds is a significant challenge. In addition, such scaffolds could be used in various therapeutic areas because of their antitumor,[8] antihypertensive,[9] and antiviral[10] activities.

With all these ideas in mind, and considering our all-out effort to develop advantageous synthetic organic transformations using novel heterogeneous catalytic systems,[11] in this article, we present the synthesis and application of 3-(propylthio)propane-1-sulfonic acid immobillized on functionalized magnetic nanoparticles [PTPSA@SiO_2–Fe_3O_4], as an environmentally-benign catalyst for the one-pot multicomponent preparation of dihydrotetrazolo[1,5-*a*]pyrimidines, dihydrotetrazolo[1,5-*a*]pyrimidine-6-carboxylates and

Department of Chemistry, Catalysis Division, University of Isfahan, Isfahan 81746-73441, Iran. E-mail: imbaltork@sci.ui.ac.ir; Fax: +98 31 3668 9732; Tel: +98 31 3793 4927

† Electronic supplementary information (ESI) available. See https://doi.org/10.1039/d2ra03813g

tetrahydrotetrazolo[5,1-*b*]quinazolinones under solvent-free conditions (Scheme 1).

Results and discussion

Preparation and characterization of [PTPSA@SiO_2–Fe_3O_4]

The preparation route for 3-(propylthio)propane-1-sulfonic acid immobilized on functionalized magnetic nanoparticles [PTPSA@SiO_2–Fe_3O_4] is displayed in Scheme 2.

First, MNPs were synthesized through a chemical co-precipitating method which is reported in the literature.[4e] Then, we used silica coating on a core particle which has several advantages of reducing the bulk conductivity and increasing the suspension stability of the core particle.[4f]

After that, a mixture of freshly-prepared SiO_2–Fe_3O_4 and (3-mercaptopropyl)trimethoxysilane (MPS) was refluxed in EtOH/H_2O for 12 hours to afford PT@SiO_2–Fe_3O_4.[12] Finally, to provide [PTPSA@SiO_2–Fe_3O_4], 1,3-propanesultone was added to a mixture of MNPs functionalized with thiopropyl groups in dry toluene, at 100 °C.

These processes were characterized by means of FT-IR, thermogravimetric analysis (TGA), SEM-EDX, elemental mapping, TEM, VSM and elemental analysis (EA).

As shown in Fig. 1a, the FT-IR spectrum of Fe_3O_4 exhibited symmetrical and asymmetrical Fe–O vibrations at 585 and 440 cm^{-1}, respectively.[11c] Additionally, a broad band, at around 3400 cm^{-1}, is assigned to the Fe–OH group.[4e,11c] The presence of bands in the FT-IR spectrum at 1100 (Si–O bonds), 3392 (stretching vibrations of Si–OH) and 798 cm^{-1} (Si–O–Fe) suggests that SiO_2 bonds well with Fe_3O_4 (Fig. 1b).[4f] As it can be seen in Fig. 1c, the characteristic bands at 2853 and 2926 cm^{-1} are attributed to the C–H stretching vibration of the linker attached on the surface of SiO_2–Fe_3O_4. Moreover, the band corresponding to SH at 2552 cm^{-1} is also evident in this spectrum. The O–C(Me) vibration observed at 900–1300 cm^{-1} (Fig. 1)

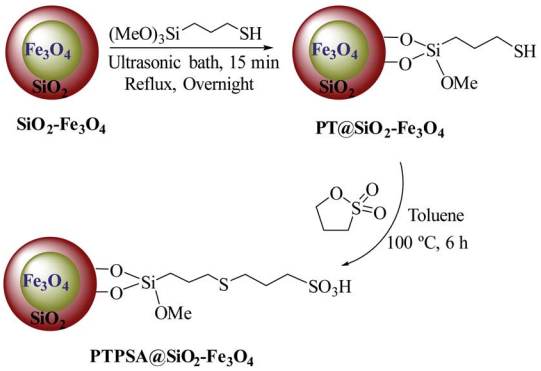

Scheme 2 Synthesis of magnetic nanocatalyst [PTPSA@SiO_2–Fe_3O_4].

(c); however, due to the presence of strong Si–O band at 1000–1100 cm^{-1}, the O–C(Me) band is masked and therefore, it is not possible to assign the O–C(Me) band appropriately. The FT-IR spectrum of Fig. 1d shows characteristic peak at around 1050–1227 cm^{-1} which is attributed to the SO_3 vibrations. The above results may indicate that these compounds have successfully been shaped on Fe_3O_4 surface.

The thermal decomposition behavior of [PTPSA@SiO_2–Fe_3O_4] between 30–700 °C, as a function of temperature, was determined by thermogravimetric analysis (TGA) (Fig. 2). In accordance with this curve, two weight loss steps were detected above 200 °C. The main weight loss is due to the removal of organic moieties (39%) on the surface. The second step (about 370–700 °C) can be attributed to the decomposition of the catalyst and production of SO_2 (around 7%). Therefore, these results proved that [PTPSA@SiO_2–Fe_3O_4] has high thermal stability.

In another analysis, SEM image of the [PTPSA@SiO_2–Fe_3O_4] showed that the particles of the nanocatalyst have sphere-like

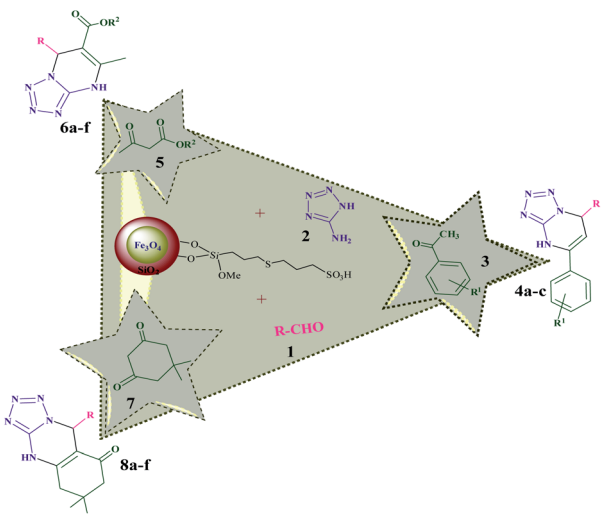

Scheme 1 One-pot synthesis of dihydrotetrazolo[1,5-*a*]pyrimidines, dihydrotetrazolo[1,5-*a*]pyrimidine-6-carboxylates and tetrahydrotetrazolo[5,1-*b*]quinazolinones.

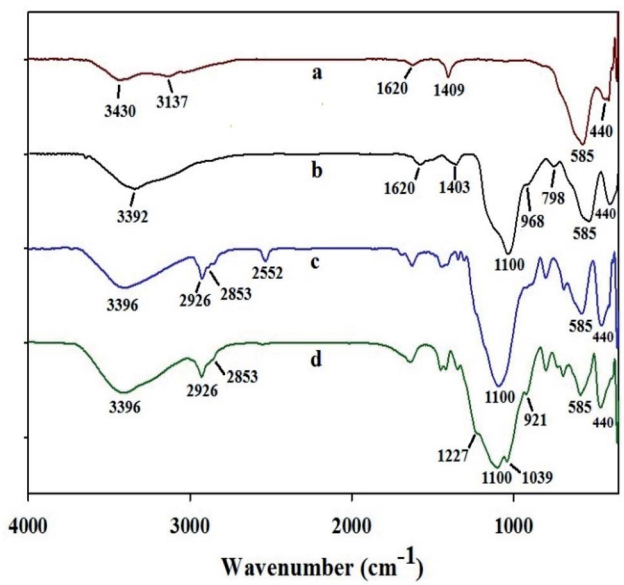

Fig. 1 Comparison of the FT-IR spectra of (a) Fe_3O_4; (b) SiO_2–Fe_3O_4; (c) PT@SiO_2–Fe_3O_4; (d) [PTPSA@SiO_2–Fe_3O_4].

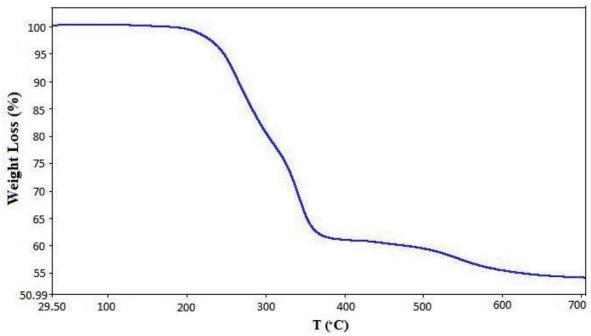

Fig. 2 TG analysis of [PTPSA@SiO_2–Fe_3O_4].

structures (Fig. 3a). Moreover, all the expected elements were confirmed by the energy dispersive X-ray (EDX) (Fig. 3b).

Further characterization of [PTPSA@SiO_2–Fe_3O_4] was performed by SEM-elemental mapping. As depicted in Fig. 4, the selected area elemental analysis indicates the presence of C, O, S, Si and Fe, which verifies good distribution and isolation of catalytic active sites for the produced catalyst.

A study done by using TEM spectroscopy (Fig. 5a–c), which is a valuable branch of knowledge to determine the morphology

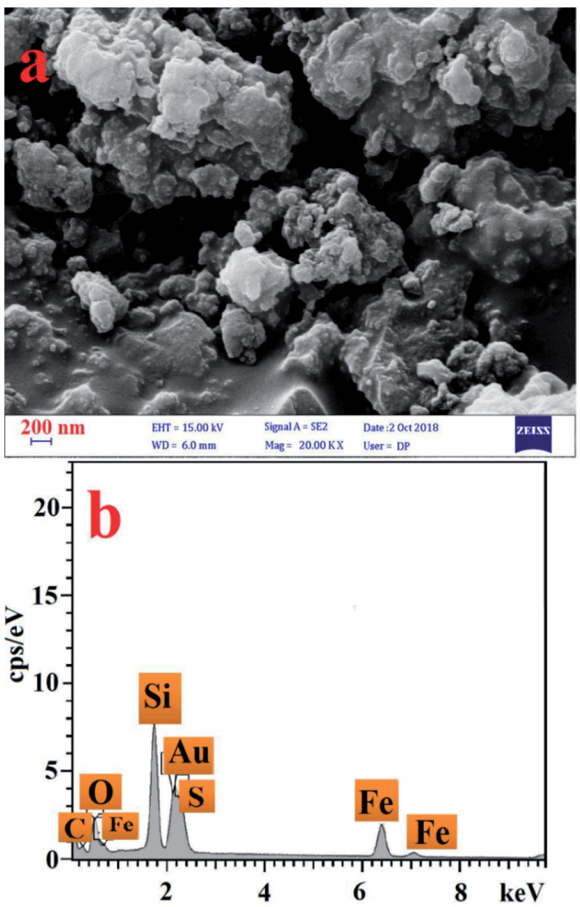

Fig. 3 (a) SEM image and (b) SEM-EDX spectrum of [PTPSA@SiO_2–Fe_3O_4].

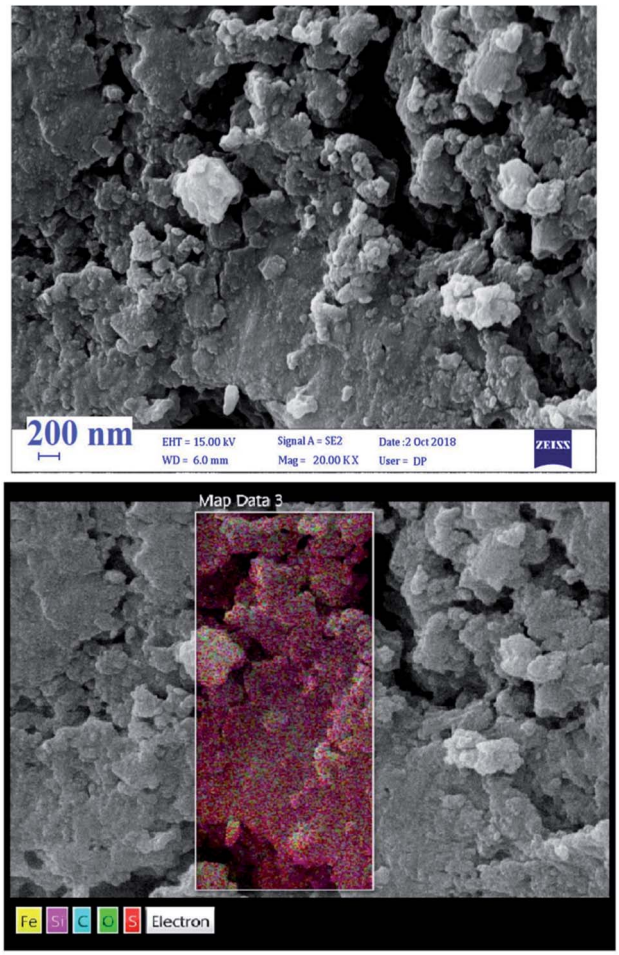

Fig. 4 Energy dispersive X-ray (EDX) mapping analysis of [PTPSA@SiO_2–Fe_3O_4].

and the size of the materials, showed well-arranged nano-spherical particles without aggregation. According to these images, particles of the catalyst were observed with a mean diameter of 3.71–11.12 nm (Fig. 5c).

As illustrated in Fig. 6, the magnetic measurements of the Fe_3O_4, SiO_2–Fe_3O_4, [PT@SiO_2–Fe_3O_4] and [PTPSA@SiO_2–Fe_3O_4] were investigated at room temperature from −8000 to +8000 Oe. The saturation magnetization (M_s) values diminished from 70 emu g^{-1} for Fe_3O_4 to 9 emu g^{-1} for the desired catalyst during the preparation route. These results indicate that the catalyst [PTPSA@SiO_2–Fe_3O_4] was successfully formed, and also, the facile separation of the magnetic catalyst from a reaction mixture was guaranteed.

The sulfur content of this nanocatalyst, is 1.52 mmol g^{-1} of the catalyst as obtained using elemental analysis.

Synthesis of dihydrotetrazolo[1,5-*a*]pyrimidine derivatives catalyzed by [PTPSA@SiO_2–Fe_3O_4]

Firstly, 4-methoxybenzaldehyde **1** (1 mmol), 5-aminotetrazole **2** (1 mmol), and acetophenone **3** (1 mmol) were adopted as the model substrates under solvent-free conditions in which no yield of the product was detected in the absence of acid catalyst

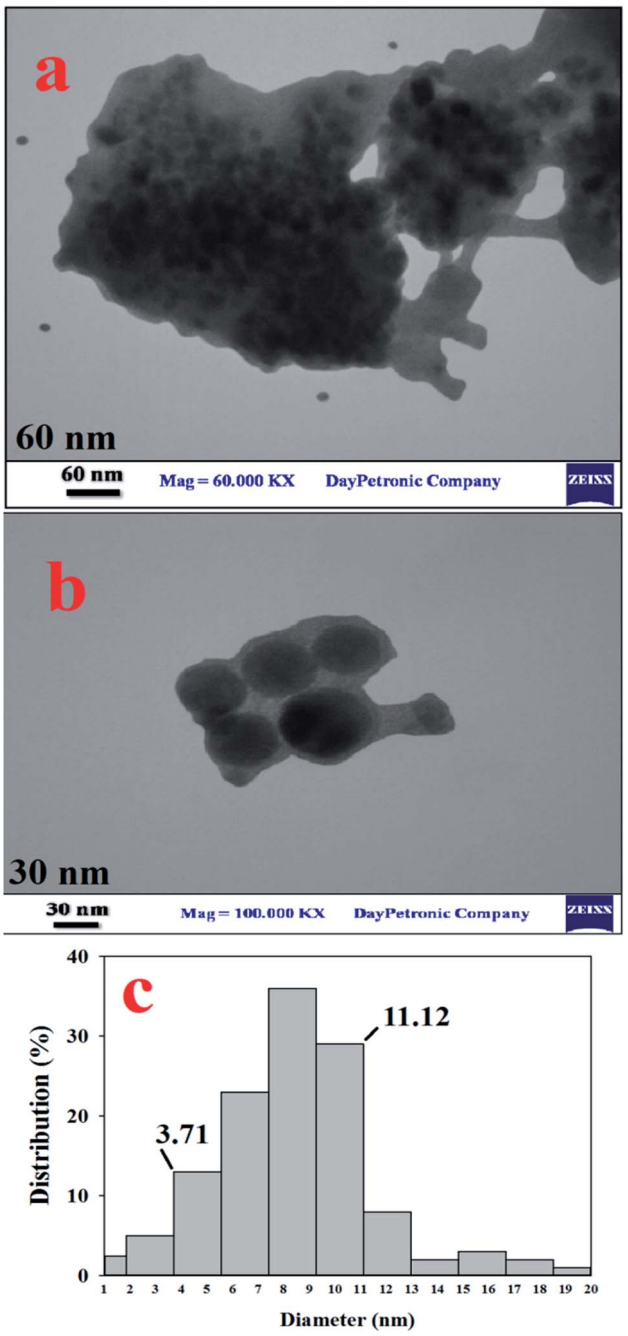

Fig. 5 TEM images in different sizes (a) 60 nm, and (b) 30 nm, and (c) particle size distribution for [PTPSA@SiO_2–Fe_3O_4].

(Table 1, entry 1). We then screened this multicomponent reaction with different acid catalysts: $ZnCl_2$, $AlCl_3$, and $FeCl_3$, to name a few (entries 2–10), and amongst them, only [PTPSA@SiO_2–Fe_3O_4] responded well to this MCR for 15 min due to its nano-character and its surface modified-SO_3H solid material compared with Fe_3O_4 (entry 10). It is noteworthy that the acidity of Fe_3O_4 with OH-groups on the surface is considerably less than [PTPSA@SiO_2–Fe_3O_4] and therefore is not effective for such a transformation (entry 8). With this catalyst, a short screening of reaction parameters including the catalyst

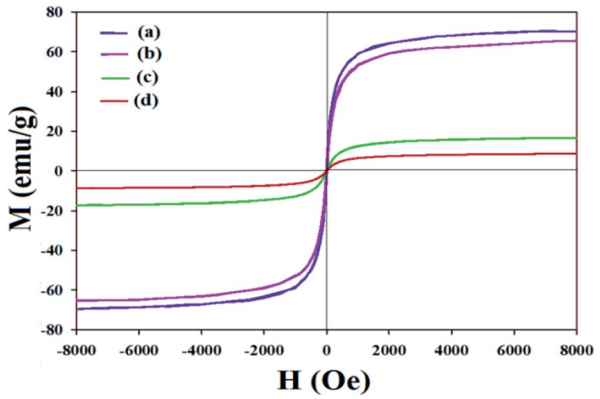

Fig. 6 Magnetization curves for (a) Fe_3O_4,[4e] (b) SiO_2–Fe_3O_4, (c) [PT@SiO_2–Fe_3O_4] and (d) [PTPSA@SiO_2–Fe_3O_4].

loading, and temperature were investigated. More precisely, different catalyst loadings were examined (entries 10–12) and gratifyingly, the desired product of **4a** was obtained with maximum yield (98%) in the presence of 5 mol% of catalyst under solvent-free conditions (entry 10). The effect of temperature, another pronounced parameter, was also tested (entries 13–15), which shows that 70 °C appeared to be the best (entry 10). As the results in Table 1 show, we fixed entry 10 as the optimal set of reaction conditions, which is the most interesting outcome of the catalyst screening for this MCR.

As shown in Scheme 3, the scope of this methodology was investigated with a set of aryl aldehydes, 5-aminotetrazole and

Table 1 Optimization studies for the synthesis of dihydrotetrazolo [1,5-*a*]pyrimidine **4a**

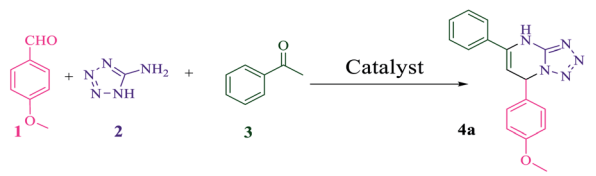

Entry	Catalyst (mol%)	T (°C)	Time (min)	Yield[a] (%)
1	—	70	60	Trace
2	$ZnCl_2$ (5)	70	15	30
3	$AlCl_3$ (5)	70	15	10
4	$FeCl_3$ (5)	70	15	15
5	$BiCl_3$ (5)	70	15	35
6	$MnCl_2$ (5)	70	15	25
7	*p*-TSA (5)	70	15	50
8	Fe_3O_4 (5)	70	15	10
9	SiO_2–Fe_3O_4 (5)	70	15	15
10	PTPSA@SiO_2–Fe_3O_4 (5)	70	15	98
11	PTPSA@SiO_2–Fe_3O_4 (3)	70	15	70
12	PTPSA@SiO_2–Fe_3O_4 (7)	70	15	98
13	PTPSA@SiO_2–Fe_3O_4 (5)	25	15	20
14	PTPSA@SiO_2–Fe_3O_4 (5)	50	15	50
15	PTPSA@SiO_2–Fe_3O_4 (5)	100	15	98

[a] Isolated yields.

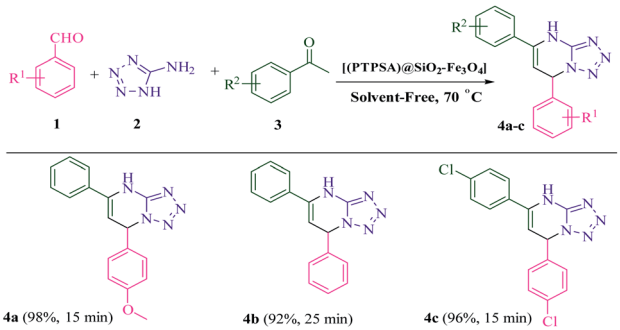

Scheme 3 Synthesis of dihydrotetrazolo[1,5-*a*]pyrimidine derivatives catalyzed by [PTPSA@SiO_2–Fe_3O_4].

acetophenone under optimal reaction conditions. To our delight, the reaction afforded dihydrotetrazolo[1,5-*a*]pyrimidines **4a–c** in excellent yields and short reaction times. Moreover, replacement of acetophenone with ethylacetoacetate was also found to be well-matched under the optimal reaction conditions (Scheme 4). Finally, all the reactions were completed in a duration of 20–30 min to afford the desired dihydrotetrazolo[1,5-*a*]pyrimidine-6-carboxylates **6a–f**. As summarized in Scheme 5, dimedone also reacted efficiently with aryl aldehydes which are substituted with methoxy, chloro and isopropyl, and 5-aminotetrazole to afford the favorite products **8a–f** in excellent yields (91–97%). Interestingly, the reaction yield with aldehyde bearing electron withdrawing groups is of comparable with that of containing electron donating ones. It seems that benzylideneacetophenone (**II**), as a strong Michael acceptor, reacts readily with 5-aminotetrazole to give an intermediate (**III**), so the reactions were completed within 20 to 30 min and the yields of the products were in the range of 88 to 98%.

Hexanal and heptanal as aliphatic aldehydes and furfural as well as 5-methyl furfural as heteroaromatic aldehydes were used in these reactions. They remained intact in the reaction mixture and no desired or side products and/or intermediates were obsereved under the identical reaction conditions even after 6 h.

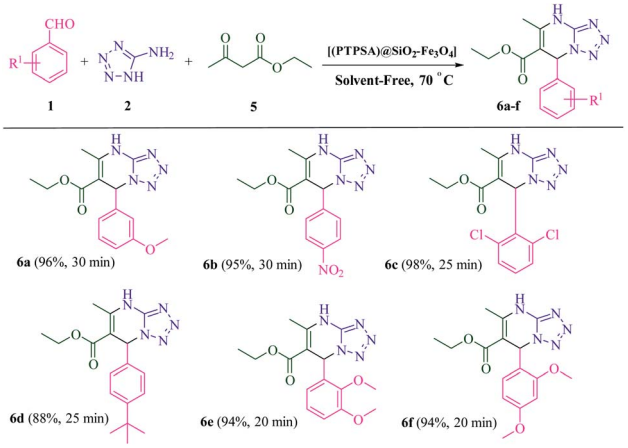

Scheme 4 Synthesis of dihydrotetrazolo[1,5-*a*]pyrimidine-6-carboxylate derivatives catalyzed by [PTPSA@SiO_2–Fe_3O_4].

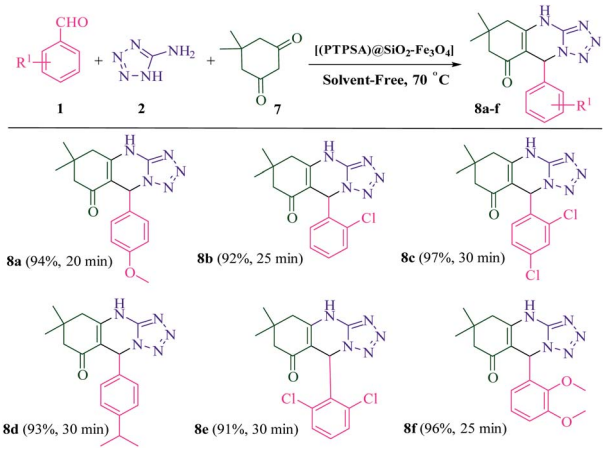

Scheme 5 Synthesis of tetrahydrotetrazolo[5,1-*b*]quinazolinone derivatives catalyzed by [PTPSA@SiO_2–Fe_3O_4].

Dihydrotetrazolo[1,5-*a*]pyrimidine derivatives were rapidly accessible on gram scales. On a 10 mmol scale, 4-methoxybenzaldehyde, reacted with 5-aminotetrazole and acetophenone in the presence of [PTPSA@SiO_2–Fe_3O_4] (0.5 mol%) at 70 °C, to give dihydrotetrazolo[1,5-*a*]pyrimidine **4a** in 70% yield after 60 min.

The structure of the products was determined from their melting points, spectral data, and elemental analysis.

A plausible mechanism for the [PTPSA@SiO_2–Fe_3O_4] catalyzed synthesis of dihydrotetrazolo[1,5-*a*]pyrimidines is represented in Scheme 6. First, the carbonyl group of aldehyde is activated by interaction of its carbonyl group with surface modified-SO_3H to give **I**. Subsequently, intermediate **I** reacts with enol form of acetophenone to give benzylideneacetophenone **II**, as a strong Michael acceptor. Then, nucleophilic attack of 5-aminotetrazole to Michael acceptor **II** provides intermediate **III**, which undergoes tautomerism to form intermediate **IV**. Lastly, an intramolecular nucleophilic attack at the keto-carbonyl site, which is followed by elimination of water in the presence of the catalyst, affords the corresponding

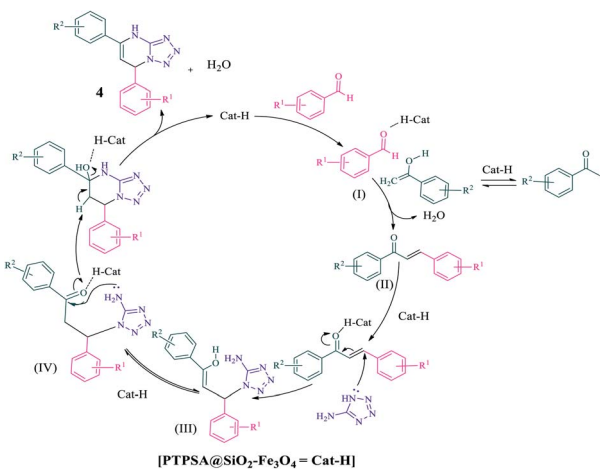

Scheme 6 Proposed reaction mechanism.

Table 2 Comparison of the results of the synthesis of **4b** catalyzed by I_2, $AlCl_3$ and [PTPSA@SiO_2–Fe_3O_4]

Catalyst/conditions	Catalyst loading	Time (h)	Yield[a] (%)	TON[b]	TOF[c] (h^{-1})	Ref.
I_2/i-PrOH, reflux	10 mol%	6	57	5.7	0.95	7a
$AlCl_3$/CH_3CN, reflux	20 mol%	4	90	4.5	1.12	7b
[PTPSA@SiO_2–Fe_3O_4]/solvent-free, 70 °C	5 mol%	0.41	92	18.4	44.87	This work

[a] Isolated yield. [b] Turn-over number. [c] Turn-over frequency.

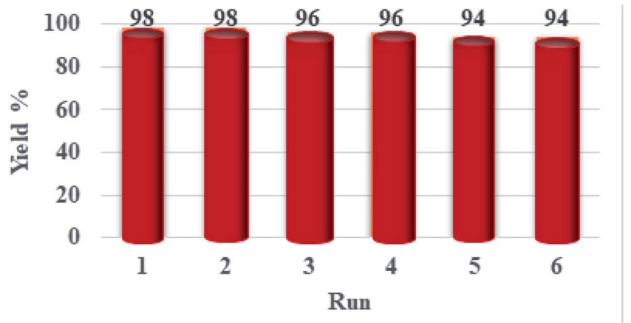

Fig. 7 Reuse of [PTPSA@SiO_2–Fe_3O_4] examined on the model reaction.

dihydrotetrazolo[1,5-*a*]pyrimidine **4** product. What is more, the catalyst is released for the next run.

To show the importance and novelty of the present work, we compared the results of our catalyst with some of those documented methods for the synthesis of similar dihydrotetrazolo [1,5-*a*]pyrimidine derivative. As can be seen, with [PTPSA@SiO_2–Fe_3O_4] catalyst the reaction time is shorter, the yield and the turn over frequency (TOF) are higher. Also the reaction conditions associated with the present method are much milder (solvent-free, 70 °C) (Table 2).

Catalyst recovery and reusability is another fantastic feature of this catalyst, which is so significant from environmental, industrial, and economic viewpoints. Therefore, the reusability of [PTPSA@SiO_2–Fe_3O_4] was explored in the synthesis of **4a** without any significant loss of its high catalytic performance for several times (Fig. 7). Later, the mixture was cooled to room temperature and diluted with cold ethanol at the end of each reaction. Finally, the catalyst was separated using an external magnet, washed with ethanol, dried and then reused for subsequent reactions. As expected, the efficiency and stability of the recovered catalyst during the synthesis of dihydrotetrazolo[1,5-*a*]pyrimidine derivative showed to be pleasing and no considerable variation after the sixth run under the reaction condition was observed (Fig. 7).

Conclusions

To summarize, we have established a novel, reusable, greatly efficient, and environmentally benign [PTPSA@SiO_2–Fe_3O_4] catalytic system for synthesis of dihydrotetrazolo[1,5-*a*]pyrimidine and tetrahydrotetrazolo[5,1-*b*]quinazolinone derivatives *via* a one-pot three-component reaction of aryl aldehyde, 5-aminotetrazole, and acetophenon derivatives/ethyl acetoacetate/dimedone under solvent-free conditions, which is undoubtedly a potential catalyst for applications in chemical industry. Significantly, the excellent magnetic recovery of this protocol gives it distinguished preference to other works done in this field.

Experimental section

General information

The chemicals used in this work were purchased from Fluka and Merck chemical companies. Melting points were determined with a Stuart Scientific SMP2 apparatus. FT-IR spectra were recorded on a Nicolet-Impact 400D spectrophotometer. ^1H and ^{13}C NMR (400 and 100 MHz) spectra were recorded on a Bruker Avance 400 MHz spectrometer using DMSO-d6 and $CDCl_3$ as solvent. Elemental analysis was performed on a LECO, CHNS-932 analyzer. Thermogravimetric analysis (TGA) was carried out on a Mettler TG50 instrument under air flow at a uniform heating rate of 20 °C min^{-1} in the range 30–700 °C. The TGA instrument was re-calibrated at frequent intervals with standards; the accuracy was always better than ±2.0%. The scanning electron microscope measurement was carried out on a Hitachi S-4700 field emission-scanning electron microscope (FE-SEM). The transmission electron microscopy (TEM) was carried out on a Philips CM10 instrument operating at 100 kV. The magnetic measurements were performed with a vibrating sample magnetometer (VSM) at Meghnatis Daghigh Kavir Co.

General procedure for preparation of [PTPSA@SiO_2–Fe_3O_4]

Preparation of [PT@SiO_2–Fe_3O_4]. First, silica-coated magnetite nanoparticles SiO_2–Fe_3O_4 (250 mg) were prepared according to the literature,[4e,f] and were continuously added to a solution of (3-mercaptopropyl)trimethoxysilane (MPS) (1 g) in 10 mL of ethanol and 10 mL of water and dispersed by sonication for 15 min and refluxed overnight. Finally, the precipitate (PT@SiO_2–Fe_3O_4) was separated by a permanent magnet, washed with water (3 × 10 mL), and dried in a vacuum oven at 50 °C.[12]

Preparation of [PTPSA@SiO_2–Fe_3O_4]. A mixture of PT@SiO_2–Fe_3O_4 (2.61 mmol, 0.196 g) and 1,3-propanesultone (2.62 mmol, 0.320 g) was intensely dispersed in 5 mL dry toluene and then, the reaction mixture was refluxed for 6 hours at 100 °C. The resulting solid was separated by a permanent magnet, washed

with toluene three times and dried under vacuum to afford [PTPSA@SiO_2–Fe_3O_4].

General procedure for synthesis of dihydrotetrazolo[1,5-*a*] pyrimidine derivatives catalyzed by [PTPSA@SiO_2–Fe_3O_4]. A mixture of aryl aldehyde (1 mmol), 5-aminotetrazole (1 mmol), acetophenone/4-chloroacetophenone (1 mmol), and [PTPSA@SiO_2–Fe_3O_4] (5 mol%, 33 mg) was stirred at 70 °C under solvent-free conditions for the duration of suitable time mentioned in Scheme 3. The progress of the reaction was monitored by TLC (eluent: petroleum ether/EtOAc, 3 : 1). Upon completion of the reaction, the mixture was cooled to room temperature and EtOH (10 mL) was added. The catalyst was quickly separated by an external magnetic field and washed with EtOH (5 mL). The products were obtained by recrystallization from EtOH and dried under reduced pressure. In some cases, the organic residue was purified by column chromatography on silica gel (petroleum ether/ethyl acetate) to provide pure products in 92–98% isolated yields (Scheme 3, **4a–c**).

General procedure for synthesis of dihydrotetrazolo[1,5-*a*] pyrimidine-6-carboxylate derivatives catalyzed by [PTPSA@SiO_2–Fe_3O_4]. A mixture of aryl aldehyde (1 mmol), 5-aminotetrazole (1 mmol), ethyl acetoacetate (1 mmol), and [PTPSA@SiO_2–Fe_3O_4] (5 mol%, 33 mg) was stirred at 70 °C under solvent-free conditions for the appropriate time indicated in Scheme 4. Upon completion, it was monitored by TLC (eluent: petroleum ether/EtOAc, 3 : 1), the work-up was done as defined for synthesis of dihydrotetrazolo[1,5-*a*]pyrimidines and the pure product was obtained in 91–98% isolated yield (Scheme 4, **6a–f**).

General procedure for synthesis of tetrahydrotetrazolo[5,1-*b*] quinazolinone derivatives catalyzed by [PTPSA@SiO_2–Fe_3O_4]. A mixture of aryl aldehyde (1 mmol), 5-aminotetrazole (1 mmol), dimedone (1 mmol), and [PTPSA@SiO_2–Fe_3O_4] (5 mol%, 33 mg) was stirred at 70 °C under solvent-free conditions for the appropriate time according to Scheme 5. The progress of the reaction was tested by TLC (eluent: petroleum ether/EtOAc, 3 : 1). After completion of the reaction, the work-up was done as described for the synthesis of dihydrotetrazolo[1,5-*a*]pyrimidines and the pure products were gained in 91–97% isolated yields (Scheme 5, **8a–f**).

Conflicts of interest

The authors declare no conflict of interest.

Abbreviations

MCR	multicomponent reaction
MNPs	magnetic nanoparticles
MPS	(3-mercaptopropyl)trimethoxysilane
p-TSA	*p*-toluenesulfonic acid
TLC	thin layer chromatography

Acknowledgements

We are grateful to the Research Council of the University of Isfahan for financial support of this work (project number 1015).

References

1 (*a*) A. Madrid, E. Pérez, M. Á. Vicente, V. Rives and R. Trujillano, *Mater*, 2022, **15**, 163–180; (*b*) S. Sun, S. Liu, F. Yu, J. Zhang, W. Xing and S. Yu, *ACS Sustainable Chem. Eng.*, 2022, **10**, 1675–1688.

2 (*a*) J. Ji, J. Yuan and Y. Wei, *Chem. Commun.*, 2022, **58**, 1601–1604; (*b*) B. Asadi, A. Landarani-Isfahani, I. Mohammadpoor-Baltork, S. Tangestaninejad, M. Moghadam, V. Mirkhani and H. Amiri Rudbari, *ACS Comb. Sci.*, 2017, **19**, 356–364; (*c*) B. Asadi, A. Landarani-Isfahani, I. Mohammadpoor-Baltork, S. Tangestaninejad, M. Moghadam, V. Mirkhani and H. Amiri Rudbari, *Tetrahedron Lett.*, 2017, **58**, 71–74; (*d*) F. G. Cirujano, R. Luque and A. Dhakshinamoorthy, *Molecules*, 2021, **26**, 1445–1451.

3 (*a*) H. Jin, B. Ruqia, Y. Park, H. J. Kim, H. S. Oh, S. I. Choi and K. Lee, *Adv. Energy Mater.*, 2021, **11**, 2003188–2003211; (*b*) B. Sarmah and R. Srivastava, *Mol. Catal.*, 2017, **427**, 62–72; (*c*) R. S. Tukhvatshin, A. S. Kucherenko, Y. V. Nelyubina and S. G. Zlotin, *ACS Catal.*, 2017, **7**, 2981–2989; (*d*) R. Kukawka, A. Pawlowska-Zygarowicz, J. Dzialkowska, M. Pietrowski, H. Maciejewski, K. Bica and M. Smiglak, *ACS Sustainable Chem. Eng.*, 2019, **7**, 4699–4706.

4 (*a*) V. Polshettiwar, R. Luque, A. Fihri, H. Zhu, M. Bouhrara and J. M. Basset, *Chem. Rev.*, 2011, **111**, 3036–3075; (*b*) L. Wu, A. Mendoza-Garcia, Q. Li and S. Sun, *Chem. Rev.*, 2016, **116**, 10473–10512; (*c*) M. Tadic, S. Kralj and L. Kopanja, *Mater. Charact.*, 2019, **148**, 123–133; (*d*) Y. Yang, J. He, Q. Li, L. Gao, J. Hu, R. Zeng, J. Qin, S. X. Wang and Q. Wang, *Nat. Nanotechnol.*, 2019, **14**, 151–156; (*e*) B. Asadi, I. Mohammadpoor-Baltork, V. Mirkhani, S. Tangestaninejad and M. Moghadam, *ChemistrySelect*, 2020, **5**, 7840–7848; (*f*) E. Estakhri, M. Nasr-Esfahani, I. Mohammadpoor-Baltork, S. Tangestaninejad, M. Moghadam and V. Mirkhani, *Appl. Organomet. Chem.*, 2017, **31**, 3799–3809; (*g*) D. Wang and D. Astruc, *Chem. Rev.*, 2014, **114**, 6949–6985.

5 (*a*) R. C. Cioc, E. Ruijter and R. V. Orru, *Green Chem.*, 2014, **16**, 2958–2975; (*b*) B. A. Neto, R. O. Rocha and M. O. Rodrigues, *Molecules*, 2022, **27**, 132–165; (*c*) H. Liu, Y. Fang, S. Y. Wang and S. J. Ji, *Org. Lett.*, 2018, **20**, 930–933; (*d*) C. Liu, L. Zhou, D. Jiang and Y. Gu, *Asian J. Org. Chem.*, 2016, **5**, 367–372; (*e*) M. Gao, M. Zou, J. Wang, Q. Tan, B. Liu and B. Xu, *Org. Lett.*, 2019, **21**, 1593–1597.

6 (*a*) L. Becan, A. Pyra, N. Rembiałkowska and I. Bryndal, *Pharmaceuticals*, 2022, **15**, 92–116; (*b*) A. U. Nerkar, *J. Adv. Chem. Sci.*, 2021, **2**, 729–732.

7 (*a*) L. Y. Zeng and C. Cai, *J. Comb. Chem.*, 2010, **12**, 35–40; (*b*) P. Kour, V. P. Singh, B. Khajuria, T. Singh and A. Kumar, *Tetrahedron Lett.*, 2017, **58**, 4179–4185; (*c*) A. Maleki, M. Niksefat, J. Rahimi and S. Azadegan, *Polyhedron*, 2019,

167, 103–110; (*d*) A. Maleki, J. Rahimi, O. M. Demchuk, A. Z. Wilczewska and R. Jasiński, *Ultrason. Sonochem.*, 2018, **43**, 262–271; (*e*) M. A. E. A. A. A. El-Remaily, A. M. Soliman, M. E. Khalifa, N. M. El-Metwaly, A. Alsoliemy, T. El-Dabea and A. M. Abu-Dief, *Appl. Organomet. Chem.*, 2021, **36**, 6320–6330; (*f*) R. Ghorbani-Vaghei, Z. Toghraei-Semiromi, M. Amiri and R. Karimi-Nami, *Mol. Diversity*, 2013, **17**, 307–318; (*g*) N. Shekarlab, R. Ghorbani-Vaghei and S. Alavinia, *J. Organomet. Chem.*, 2021, **949**, 121971–121980.

8 E. Wagner, K. Al-Kadasi, M. Zimecki and W. Sawka-Dobrowolska, *Eur. J. Med. Chem.*, 2008, **43**, 2498–2504.

9 O. Alam, S. A. Khan, N. Siddiqui, W. Ahsan, S. P. Verma and S. J. Gilani, *Eur. J. Med. Chem.*, 2010, **45**, 5113–5119.

10 J. Balzarini and C. McGuigan, *J. Antimicrob. Chemother.*, 2002, **50**, 5–9.

11 (*a*) M. Samadani, B. Asadi, I. Mohammadpoor-Baltork, V. Mirkhani, S. Tangestaninejad and M. Moghadam, *RSC Adv.*, 2021, **11**, 11976–11983; (*b*) M. Azizi, M. Nasr-Esfahani, I. Mohammadpoor-Baltork, M. Moghadam, V. Mirkhani, S. Tangestaninejad and R. Kia, *J. Org. Chem.*, 2018, **83**, 14743–14750; (*c*) B. Asadi, I. Mohammadpoor-Baltork, S. Tangestaninejad, M. Moghadam, V. Mirkhani and A. Landarani-Isfahani, *New J. Chem.*, 2016, **40**, 6171–6184; (*d*) T. Ataee-Kachouei, M. Nasr-Esfahani, I. Mohammadpoor-Baltork, V. Mirkhani, M. Moghadam, S. Tangestaninejad and B. Notash, *Appl. Organomet. Chem.*, 2020, **34**, 5948–5965.

12 C. S. Gill, B. A. Price and C. W. Jones, *J. Catal.*, 2007, **251**, 145–152.